

JAERI-M

8 0 8 8

SOURCE PLASMA STUDY OF THE
DUOPIGATRON ION SOURCE FOR JT-60
NEUTRAL BEAM INJECTOR

February 1979

Yoshihiro ARAKAWA, Masato AKIBA*, Umeo KONDOH,**
Shinzaburo MATSUDA and Tokumichi OHGA

この報告書は、日本原子力研究所が JAERI-M レポートとして、不定期に刊行している研究報告書です。入手、複製などのお問い合わせは、日本原子力研究所技術情報部（茨城県那珂郡東海村）あて、お申しこしください。

JAERI-M reports, issued irregularly, describe the results of research works carried out in JAERI. Inquiries about the availability of reports and their reproduction should be addressed to Division of Technical Information, Japan Atomic Energy Research Institute, Tokai-mura, Naka-gun, Ibaraki-ken, Japan.

Source Plasma Study of the DuoPIGatron Ion
Source for JT-60 Neutral Beam Injector

Yoshihiro ARAKAWA, Masato AKIBA*, Umeo KONDOH,**

Shinzaburo MATSUDA and Tokumichi OHGA

Division of Thermonuclear Fusion Research,
Tokai Research Establishment, JAERI

(Received January 18, 1979)

In an effort to develop a plasma source capable of producing a dense, uniform, and quiescent plasma for JT-60 neutral beam injectors, experimental studies on duoPIGatron ion sources have been pursued. In the 15 cm axisymmetric duoPIGatron ion source, the ion current density is about 250 mA/cm^2 , uniform to $\pm 10\%$ over the extraction grid. In the rectangular duoPIGatron source, the ion current is 190 mA/cm^2 , uniform to $\pm 5\%$ over the area of 8 cm by 24 cm. By measuring potential distributions of the source plasma, we have found the fact that copper buttons located at downstream of the intermediate electrode play an important role in raising the density level, gas efficiency, and arc efficiency as well as in improving the plasma uniformity.

Keywords: Source Plasma, DuoPIGatron Ion Source, Neutral Beam Injector, Duoplasmatron, Cusp, Current Density, Plasma Uniformity

*) On leave from Kyushu University

**) On leave from Nissin Electric Co., Ltd

JT-60中性粒子入射装置用デュオピガトン型
イオン源のソースプラズマ

日本原子力研究所東海研究所核融合研究部

荒川義博・秋場真人^{*}・近藤梅夫^{**}

松田慎三郎・大賀徳道

(1979年1月18日受理)

JT-60中性粒子入射装置用イオン源を開発するため、デュオピガトン型イオン源を用いてソースプラズマの改良実験をおこなった。円形デュオピガトン型イオン源（引出し電極：1.5 cm ϕ ）では、引出し電極面全面にわたって一様（密度変化 $\pm 10\%$ 以内）かつ高密度（イオン飽和電流密度；250 mA/cm²）なソースプラズマが得られた。又矩形デュオピガトン型イオン源（引出し電極；1.2 cm \times 2.7 cm）では、引出し電極面の一部（8 cm \times 2.4 cm）で一様（密度変化 $\pm 5\%$ 以内）で、イオン飽和電流密度190 mA/cm²のソースプラズマが得られた。

* 特別研究生 九州大学

** 外来研究員 日新電機

Contents

1. Introduction	1
2. Apparatus and Experimental Procedure	2
3. Results and Discussion	2
4. Concluding Remarks	7
Acknowledgement	8
References	9
Figures	10

目 次

1	はじめに	1
2	実験装置及び方法	2
3	実験結果及び考察	2
4	結 論	7
	謝 辞	8
	参考文献	9
	☒	10

§1. Introduction

Ion Sources for JT-60 neutral beam injector are required to produce well-collimated, high current ion beams with an ion current density of 0.27 A/cm^2 through the $12 \text{ cm} \times 27 \text{ cm}$ rectangular extraction grid.¹⁾ To this end, the plasma source should be capable of producing a dense, uniform, and quiescent plasma over the large extraction grid. Both noise level and spatial density variations should be below $\pm 10 \%$ over the extraction area at the above density level. (an ion saturation current density of 0.27 A/cm^2) Besides, the plasma source should have high gas efficiency to reduce gas load to the pumping system.

For this purpose, we have undertaken experiments using duoPIGatron ion sources originally developed at Oak Ridge National Laboratory.²⁾³⁾ Our prototype ion source, employed for JFT-2 neutral beam injector, had the extraction grid diameter of 7 cm and produced a maximum drain current of 8 A at 25-30 kV.⁴⁾ For the increase of the drain current, the first modification was the geometrical scale up of extraction grids to 15 cm diameter together with uses of axial buttons located at downstream of the intermediate electrode and of a set of line cusp confinement magnets around the arc chamber wall. The second modification is the further geometrical scale up of the extraction grids to a rectangular 12 cm by 27 cm grids using buttons and multipole confinement magnets. With this rectangular-shaped ion source, we have taken an effort to improve the source plasma by trying to use several size of buttons and cusp configuration.

§2. Apparatus and Experimental Procedure

In this experiment, we have used two types of duoPIGatron ion sources. The one is the source with a 15 cm grid diameter, the other with a rectangular-shaped grid, 12 cm by 27 cm.

Figures 1 and 2 are the sketches of the axisymmetric 15 cm diam. ion source and rectangular source, respectively. The former has a 14 mm diam. copper button located axially at 2.5 cm downstream of the intermediate electrode and has a set of line cusp confinement magnets. The latter has the copper button shown in Fig. 3 and is equipped with one of two types of magnetic multipole arrangements. The one is the line cusp, the other is the point cusp. Each magnet used in both circular and rectangular ion sources, which is made of samarium-cobalt, produces a field strength of 4 kG at the pole surface.

Density of the source plasma was measured by Langmuir probes located 0.5 cm above the target cathode*. The axial density gradient toward the target cathode was also measured by the separate axially movable probe.

In addition, single and double probes were set in the intermediate electrode chamber to measure the electron temperatures, densities, and space potential of the cathode plasma.

§3. Results and Discussion

Figure 4 shows a typical example of the density profiles of the source plasma in the 15 cm diam. duoPIGatron ion source prior to improvement. Ion saturation current is measured by the Langmuir probe at 2.5 cm above the target cathode. Uniformity can be improved by lowering the magnetic field

*) Results obtained in Figs. 4, 5, 7 and 10 were measured at the different probe position, about 2.5 cm above the target cathode.

§2. Apparatus and Experimental Procedure

In this experiment, we have used two types of duoPIGatron ion sources. The one is the source with a 15 cm grid diameter, the other with a rectangular-shaped grid, 12 cm by 27 cm.

Figures 1 and 2 are the sketches of the axisymmetric 15 cm diam. ion source and rectangular source, respectively. The former has a 14 mm diam. copper button located axially at 2.5 cm downstream of the intermediate electrode and has a set of line cusp confinement magnets. The latter has the copper button shown in Fig. 3 and is equipped with one of two types of magnetic multipole arrangements. The one is the line cusp, the other is the point cusp. Each magnet used in both circular and rectangular ion sources, which is made of samarium-cobalt, produces a field strength of 4 kG at the pole surface.

Density of the source plasma was measured by Langmuir probes located 0.5 cm above the target cathode*. The axial density gradient toward the target cathode was also measured by the separate axially movable probe.

In addition, single and double probes were set in the intermediate electrode chamber to measure the electron temperatures, densities, and space potential of the cathode plasma.

§3. Results and Discussion

Figure 4 shows a typical example of the density profiles of the source plasma in the 15 cm diam. duoPIGatron ion source prior to improvement. Ion saturation current is measured by the Langmuir probe at 2.5 cm above the target cathode. Uniformity can be improved by lowering the magnetic field

*) Results obtained in Figs. 4,5,7 and 10 were measured at the different probe position, about 2.5 cm above the target cathode.

intensity formed by the solenoidal coil, but the density becomes too low to produce high-current ion beams. This may be that the diffusion loss of the charged particles from the PIG plasma to the chamber walls is increased with lowering the magnetic field.

As a first step of improvements of the source plasma, we tried to use an axial copper button located at about 2.5 cm downstream of the intermediate electrode snout. Its effect is shown in Fig. 5. It is seen that the source plasma uniformity is improved without lowering the density level by the use of the button of optimum size. However it cannot be improved without impairing the density level by the use of the button of larger size. It has been already reported⁵⁾ that an axial button can improve plasma uniformity without impairing the density level, for the reason that it reduces the passage of current carrying electrons, thereby intensifies the PIG discharge by increasing the kinetic energy of ionizing electrons as they travel across the double sheath. The widened plasma production area by diverting the arc column from on-axis to off axis also contributes to the uniform density distribution.

Instead of the button, we have also used the duoplasmatron with a center pole shown in Fig. 6. This center pole which is water-cooled and axially movable, can vary the passage of ionizing electrons, diverting from on-axis to off-axis, and lead to the PIG plasma. Its effect is the same as that of button located at downstream of the intermediate electrode. Figure 7 shows variations of the density profile with position of the center pole, where Z denotes the axial position of the pole tip relative to the intermediate electrode snout. It is seen that the density profile is improved, especially in the density level, by locating the center pole downstream.

Figure 8 shows a typical example of an axial potential distribution

in the duoPIGatron ion source. It is seen that the source plasma is composed of a cathode plasma and a PIG plasma separated by a double sheath. The potential of the cathode plasma can be estimated from the potential of the baffle (or intermediate electrode) and the electron temperature. This electron temperature is measured by a double probe, set in the intermediate electrode region, in the range of 2-4 eV in the present experimental conditions.

Figure 9 shows potential variations of the anode, PIG plasma, target cathode, baffle and cathode plasma relative to the filament cathode with position of the center pole. From this figure, it is seen that the potential jump across the double sheath which is the potential difference between the cathode plasma and the PIG plasma, is raised enough to explain the increase of the plasma density as the center pole is displaced downstream. Because higher energy of the ionizing electrons through the double sheath contributes more effectively to an increase of the production rate of the PIG plasma in the present energy level. In addition, it is seen that the anode fall, which is equal to the potential difference between anode and PIG plasma, decreases significantly as the center pole is displaced downstream. This corresponds to the improved arc thermal efficiency, because the heat loss to the anode is reduced in proportion to a decrease of the anode fall.

As a second step of the improvement of the source plasma, the potential of the arc chamber was varied by changing the electrical cable connection to the electrodes shown in Fig. 10. In the case of (A), the arc chamber wall is directly connected to the target cathode. They are floated by being connected to the positive terminal of the arc power supply through a resistor of 200 ohm. In this case, a typical density profile of the source plasma is shown by the broken line. In the case of (B), the chamber wall

is connected to the positive terminal through the resistor of R and is not in the same potential as the target cathode. In this case, the wall potential is equal to or positive with respect to the space potential of the source plasma when a small value of R is chosen. Once this occurs, the wall loss of the charged particles decreases and both density level and plasma uniformity become improved as seen in Fig. 10.

Undergoing the experiment, we have found that there is a significant density gradient near the target cathode as seen in Fig. 11 when the target cathode is at a floating potential, as labeled FLOAT or at more negative potential against the space potential of the source plasma i.e., when the target cathode is connected to the negative terminal, labeled FILAMENT. Only a small density gradient is observed when one electrically connects the target cathode to the anode, that is short out the PIG, labeled ANODE. This fact indicates that the density gradient is caused by the diffusion loss of the charged particles to the target cathode.⁶⁾ Because this diffusion loss rate is larger in the former case than in the latter case due to the difference of directional velocity of ions to the target cathode.*

Figure 12 shows the density profiles of the source plasma with the

*) In the former case, the directional velocity is equal to the sound velocity v_s given by

$$v_s = \sqrt{\frac{kT_e}{M}}$$

where T_e is the electron temperature, M the ion mass.

In the latter case, the directional velocity is equal to the thermal ion velocity v_{th} given by

$$v_{th} = \sqrt{\frac{8kT_i}{\pi M}}$$

where T_i is the ion temperature. Since $T_e \gg T_i$, v_s is larger than v_{th} .

14 mm diam. button and line cusp confinement. In this case, the arc chamber wall is directly connected to the positive terminal. The plasma density is measured by a Langmuir probe located 0.5 cm above the target cathode. As seen in this figure, the ion current density is up to 0.25 A/cm^2 , uniform to $\pm 10\%$ over the 15 cm grid diameter at an arc current of 305 A.

As the high energy ion source is planned to use at present for JT-60 injectors, we have made the rectangular duoPIGatron ion source. To produce high-current, low divergent ion beams, it is necessary to generate a dense plasma while maintaining spatial uniformity. To make the source plasma uniform in the longitudinal direction of the rectangular grid, we have made two types of duoPIGatron ion sources. The one has two duoplasmatrons with circular-shaped nozzle snout, the other has one duoplasmatron with slot-shaped nozzle snout as shown in Figs. 13 and 2, respectively.

In the former source, a typical example of density profiles is shown in Fig. 14, where Y denotes the distance from the center in the longitudinal direction of the extraction grid. It is seen that there are two peaks in the density profiles caused by two duoplasmatrons. In order to flatten the density profile, copper buttons is located at 2.5 cm downstream of each intermediate electrode. This effect is seen in Fig. 15. Source plasma uniformity can be improved to some extent, but the density level obtained is too low to produce high-current ion beams unless an arc current would be increased more than 1000 A. Therefore it would be quite difficult to obtain our planned density level.

In the latter case, a typical example of the density profiles in the transverse and longitudinal directions are shown in Figs. 16 and 17, respectively. In these figures, X and Y denote the distance from the center of the grid in the transverse and longitudinal directions, respectively. In this case, a copper slot-shaped button is located at

downstream of the intermediate electrode. Point cusp confinement magnets are set around the chamber walls, too. This magnetic configuration is originally used by Mackenzie and his CO-workers.⁷⁾ A comparison of the density profiles is also made between two cases, when working gas is fed only into the intermediate electrode chamber, denoted by NORMAL GAS FEED and when working gases are supplied into both the intermediate electrode chamber and the PIG chamber, denoted by NORMAL PLUS EXTRA GAS FEED. Source plasma uniformity, especially in the longitudinal direction, is improved by operating with the proper combination of these gas feeds.

To boost the plasma density at a fixed arc current, it is necessary to make use of magnetic confinement around the chamber walls in order to confine energetic ionizing electrons and reduce the wall loss of charged particles. The effect of the point cusp arrangement is shown in Figs. 18 and 19. The plasma density is increased by about 30 % by the use of point cusp confinement, but source plasma uniformity is not appreciably improved as expected. The reason is considered as follows. The nozzle snout of this source is too narrow to diffuse the ionizing electrons into the PIG region. Therefore the plasma production is lacking near the chamber walls.

Figure 20 shows the density profiles of the source plasma in the transverse direction with the button and point cusp confinement. The ion saturation current density reaches 0.19 A/cm^2 , uniform to $\pm 5 \%$ over the area of 8 cm by 24 cm at an arc current of 340 A.

§4. Concluding Remarks

We have undertaken the experiment to improve the source plasmas of the 15 cm diam. axisymmetric source and rectangularly-shaped source. From the

downstream of the intermediate electrode. Point cusp confinement magnets are set around the chamber walls, too. This magnetic configuration is originally used by Mackenzie and his CO-workers.⁷⁾ A comparison of the density profiles is also made between two cases, when working gas is fed only into the intermediate electrode chamber, denoted by NORMAL GAS FEED and when working gases are supplied into both the intermediate electrode chamber and the PIG chamber, denoted by NORMAL PLUS EXTRA GAS FEED. Source plasma uniformity, especially in the longitudinal direction, is improved by operating with the proper combination of these gas feeds.

To boost the plasma density at a fixed arc current, it is necessary to make use of magnetic confinement around the chamber walls in order to confine energetic ionizing electrons and reduce the wall loss of charged particles. The effect of the point cusp arrangement is shown in Figs. 18 and 19. The plasma density is increased by about 30 % by the use of point cusp confinement, but source plasma uniformity is not appreciably improved as expected. The reason is considered as follows. The nozzle snout of this source is too narrow to diffuse the ionizing electrons into the PIG region. Therefore the plasma production is lacking near the chamber walls.

Figure 20 shows the density profiles of the source plasma in the transverse direction with the button and point cusp confinement. The ion saturation current density reaches 0.19 A/cm^2 , uniform to $\pm 5 \%$ over the area of 8 cm by 24 cm at an arc current of 340 A.

§4. Concluding Remarks

We have undertaken the experiment to improve the source plasmas of the 15 cm diam. axisymmetric source and rectangularly-shaped source. From the

experimental results, we have obtained the concluding remarks;

1. In the axisymmetric duoPIGatron ion source with a grid diameter of 15 cm, the ion current density is increased up to 0.25 A/cm^2 , uniform to $\pm 10\%$ over the extraction grid.
2. In the rectangular duoPIGatron source, the ion current density is increased up to 0.19 A/cm^2 , uniform to $\pm 5\%$ over the $8 \text{ cm} \times 24 \text{ cm}$ area at an arc current of 340 A.
3. It was found that buttons located at downstream of the nozzle snout not only improve the spatial uniformity of the source plasma, but also elevate the density level and arc efficiency.
4. Density gradient of the source plasma generated near the target cathode, usually observed, was caused by the diffusion loss of the charged particles.

Acknowledgement

The authors would like to express their appreciations to Drs. H. Shirakata and T. Sugawara for their valuable discussions. Thanks are also due to Drs. S. Mori and Y. Obata for their support and encouragement.

experimental results, we have obtained the concluding remarks;

1. In the axisymmetric duoPIGatron ion source with a grid diameter of 15 cm, the ion current density is increased up to 0.25 A/cm^2 , uniform to $\pm 10 \%$ over the extraction grid.
2. In the rectangular duoPIGatron source, the ion current density is increased up to 0.19 A/cm^2 , uniform to $\pm 5 \%$ over the $8 \text{ cm} \times 24 \text{ cm}$ area at an arc current of 340 A.
3. It was found that buttons located at downstream of the nozzle snout not only improve the spatial uniformity of the source plasma, but also elevate the density level and arc efficiency.
4. Density gradient of the source plasma generated near the target cathode, usually observed, was caused by the diffusion loss of the charged particles.

Acknowledgement

The authors would like to express their appreciations to Drs. H. Shirakata and T. Sugawara for their valuable discussions. Thanks are also due to Drs. S. Mori and Y. Obata for their support and encouragement.

References

- 1) S. Matsuda et al.; JAERI-M 7655 (1978)
- 2) W.L. Stirling et al.; ORNL/TM-5662 (1976)
- 3) C.C. Tsai et al.; 7th Symp. on Engineering Problems of Fusion Research (1977)
- 4) T. Sugawara et al.; JAERI-M 7043 (1977)
- 5) R.C. Davis et al.; ORNL/TM-4657 (1974)
- 6) Y. Arakawa et al.; to be published
- 7) R. Limpaecher and K.R. Mackenzie; Rev. Sci. Instrum., 44 (1973)

727

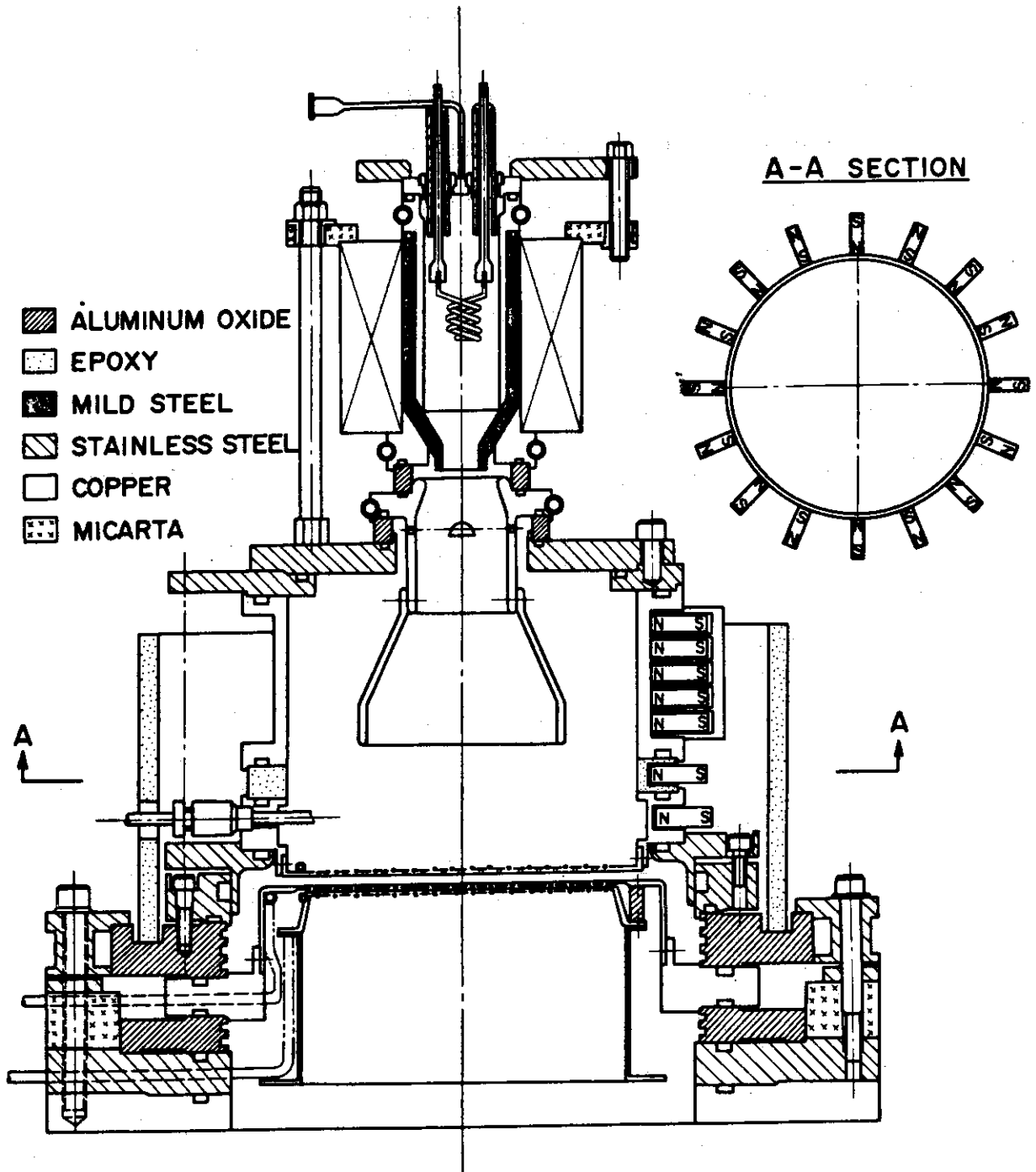


Fig. 1 Schematic of the 15 cm diam. duoPIGatron ion source with a button and line cusp confinement.

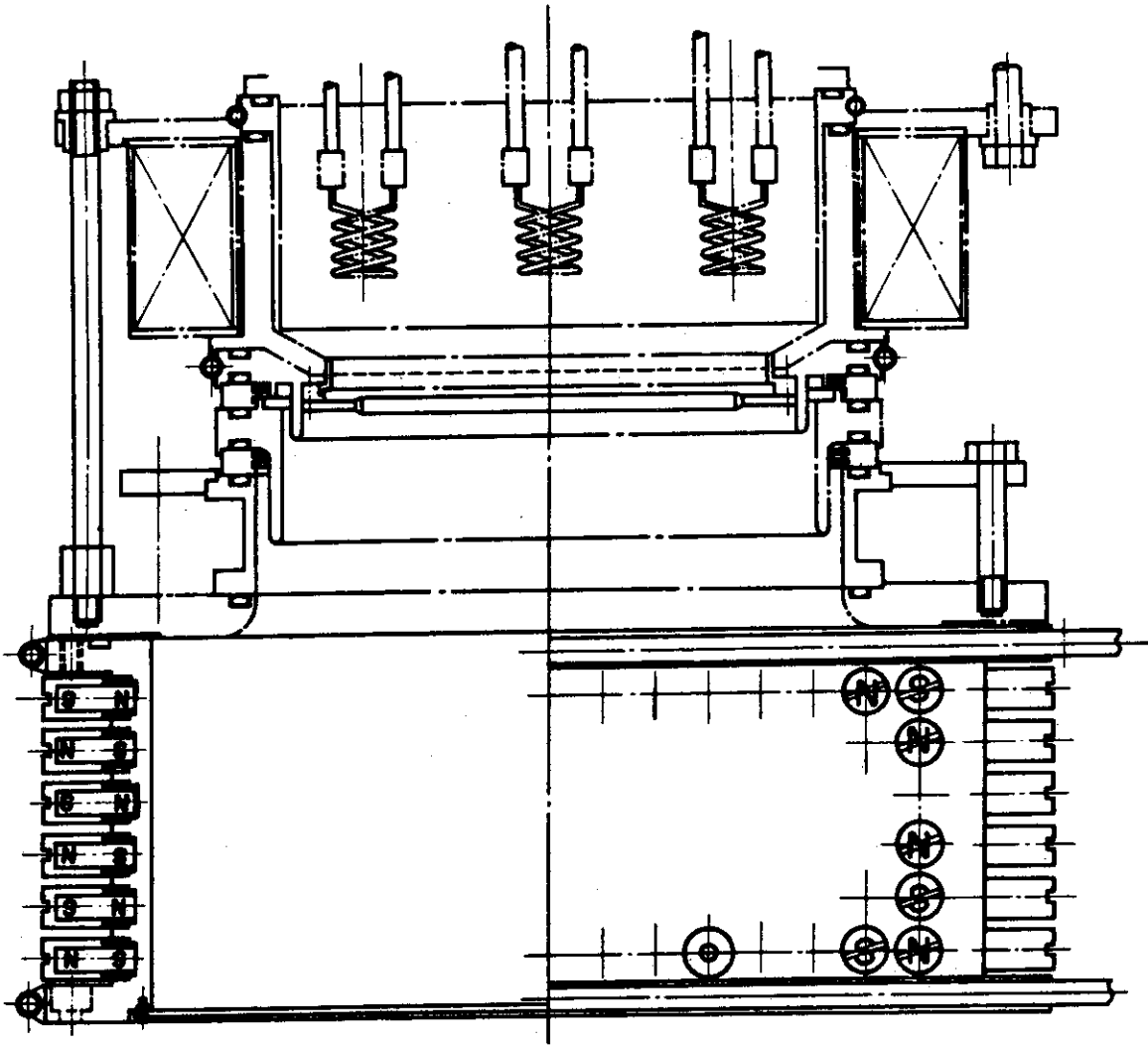


Fig. 2 Schematic of the rectangular duoPIGatron source with a button and point cusp confinement.

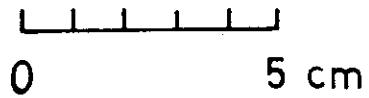
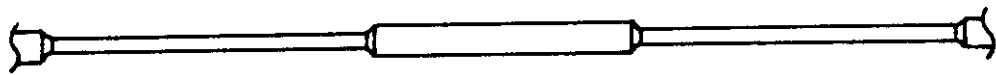


Fig. 3 Copper button used in the rectangular duoPIGatron source.

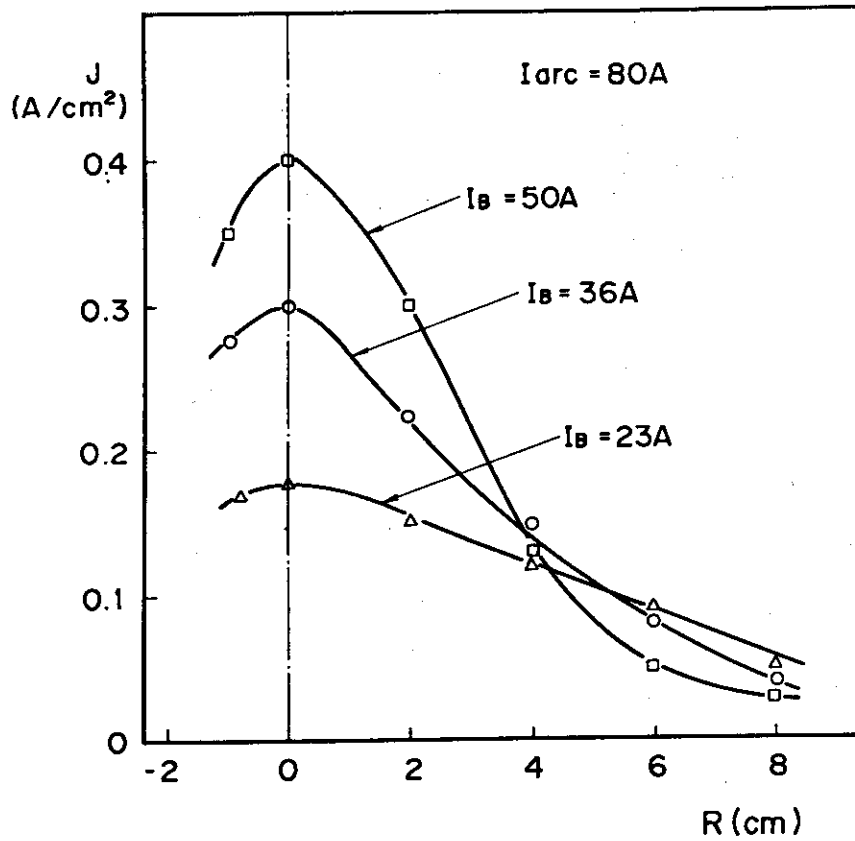


Fig. 4 Density profiles of the source plasma before improvement, where J is ion saturation current density, I_{arc} arc current, I_B coil current, R radial position.

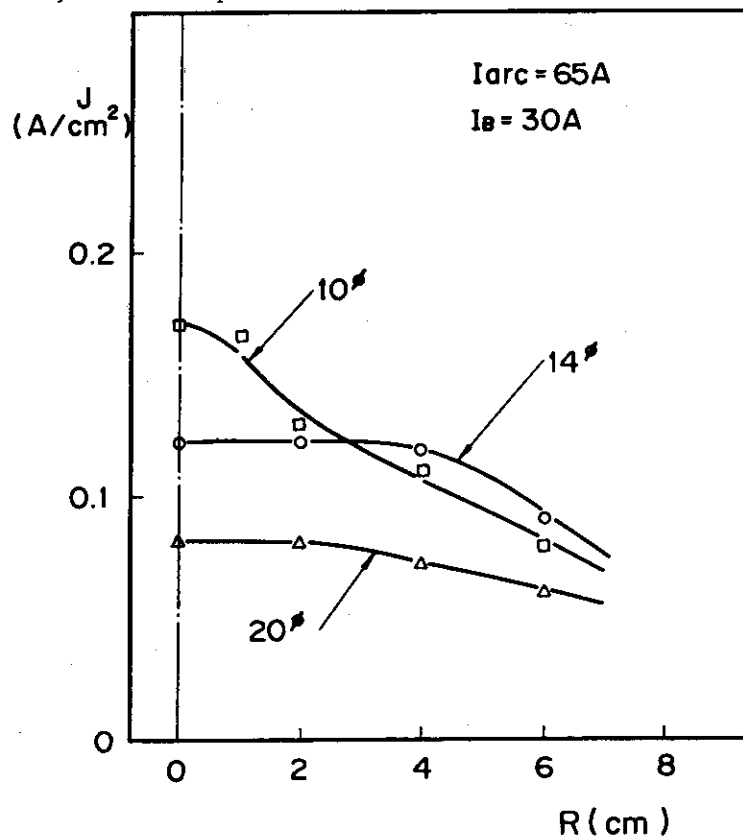


Fig. 5 Variations of the density profile with size of a button.

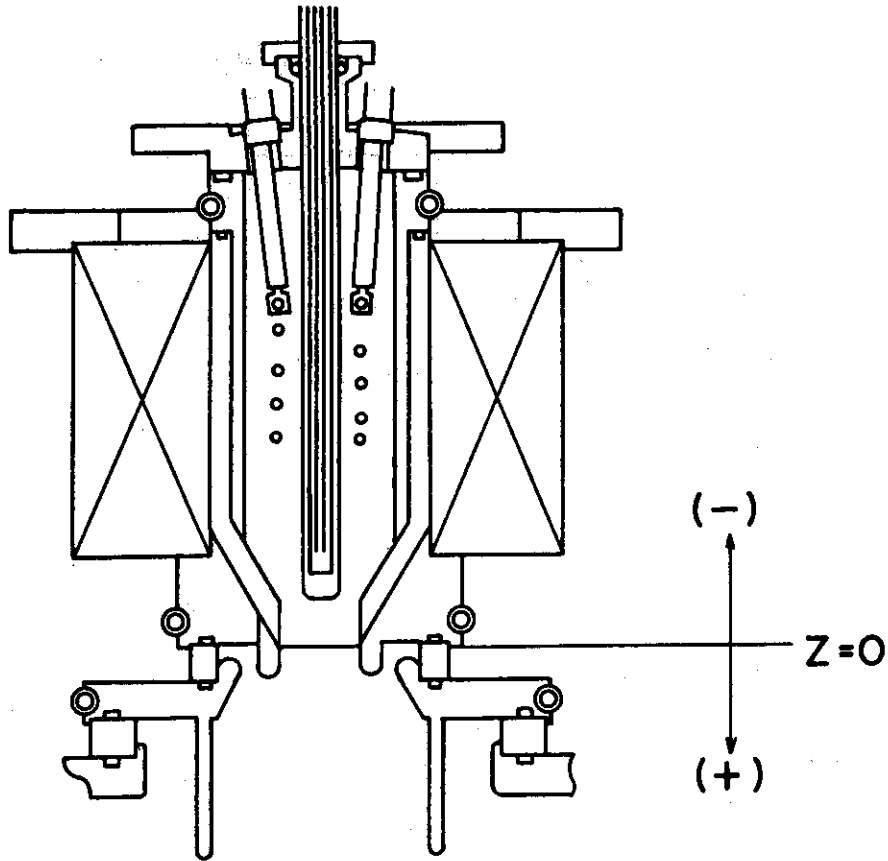


Fig. 6 Duoplasmatron with a center pole.

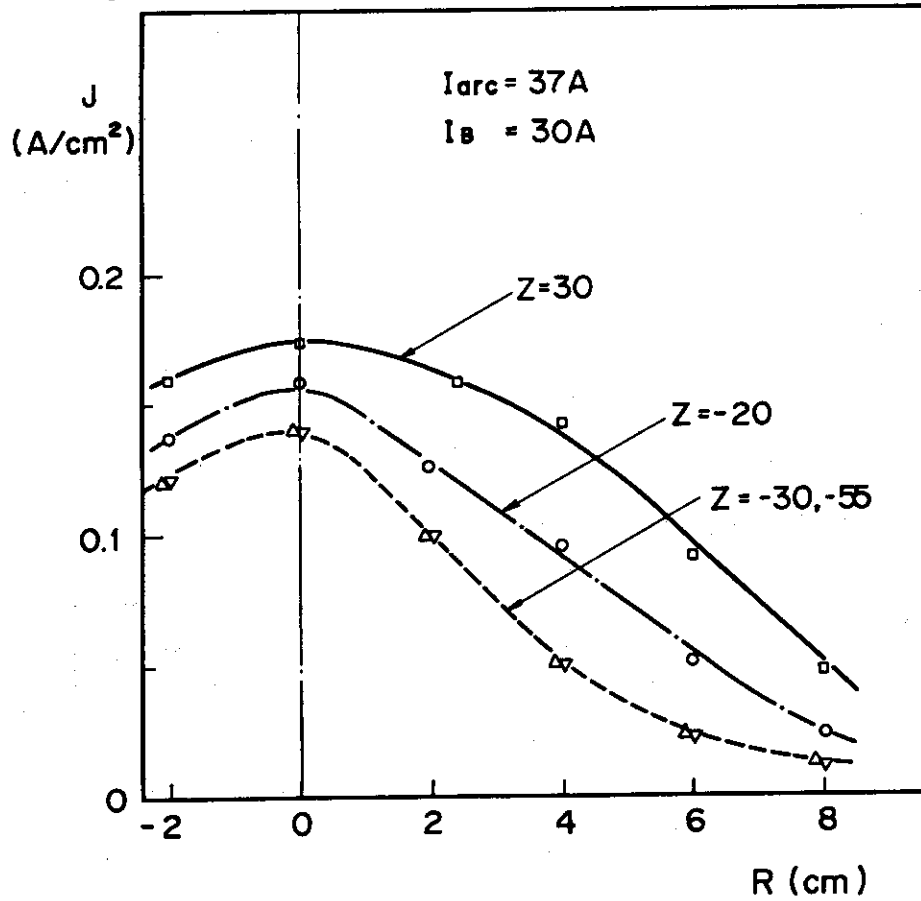


Fig. 7 Variations of the density profile with position of the center pole.

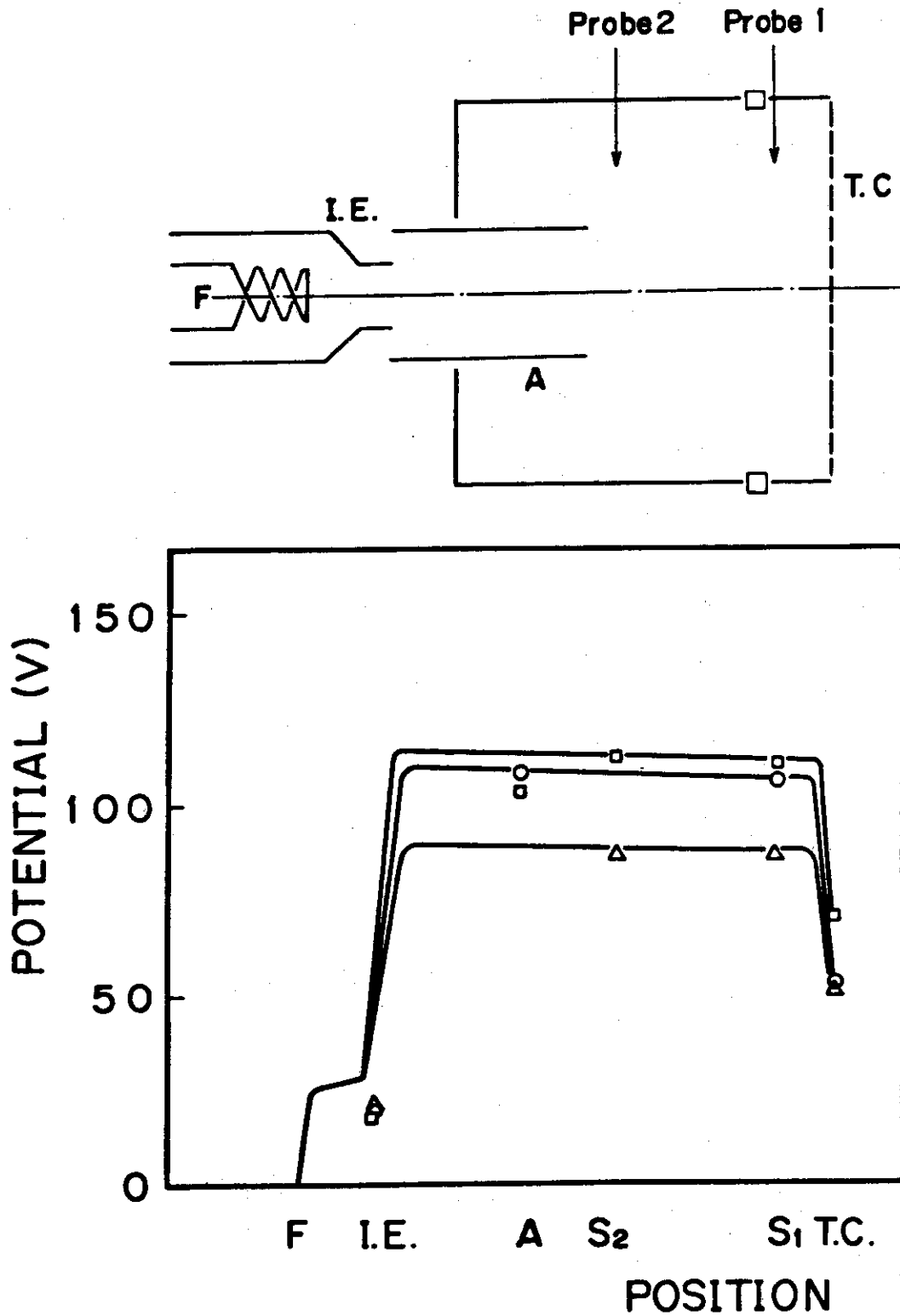


Fig. 8 Axial potential distributions in the duoPIGatron source.

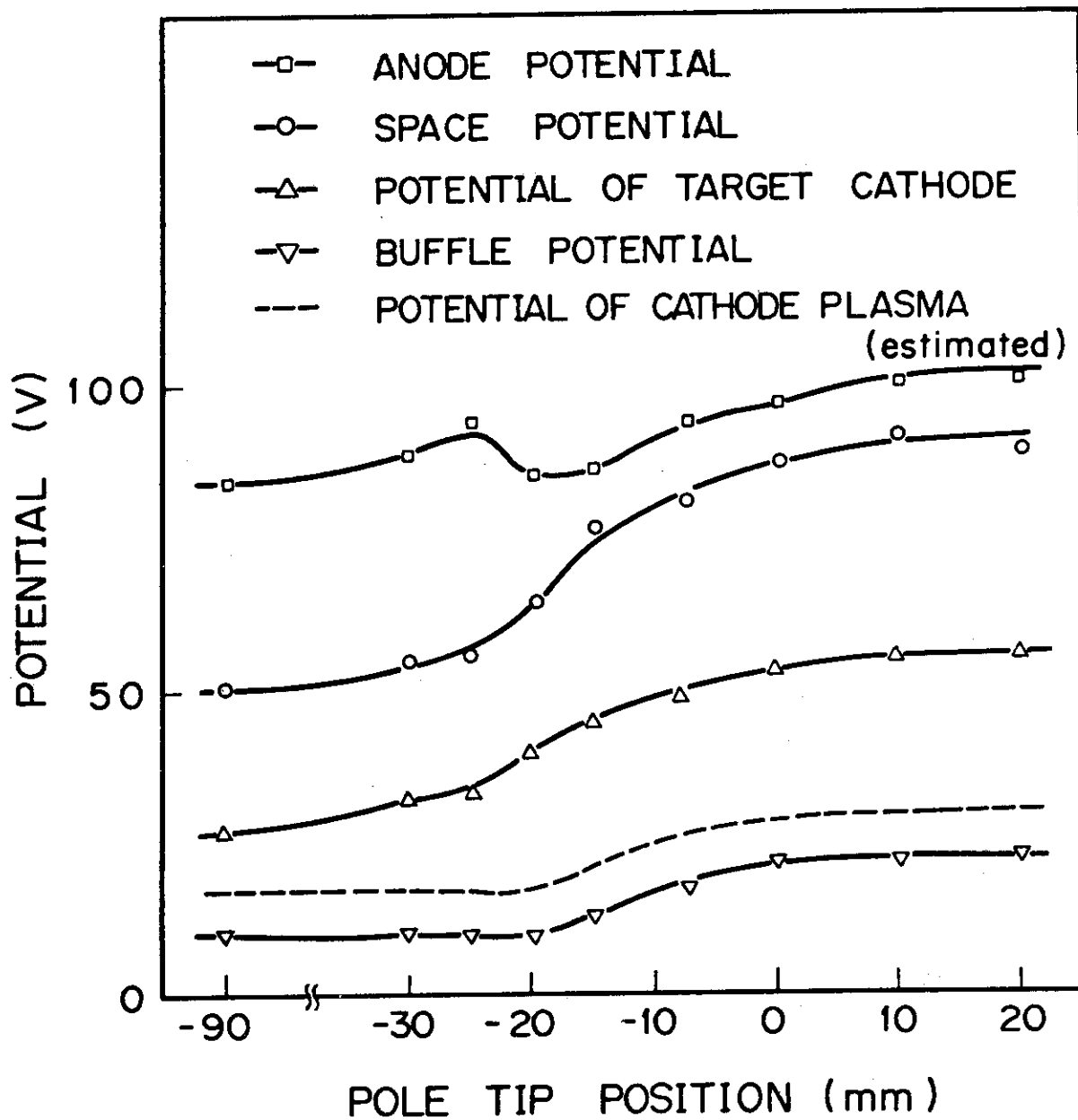


Fig. 9 Potential variations with position of the center pole.

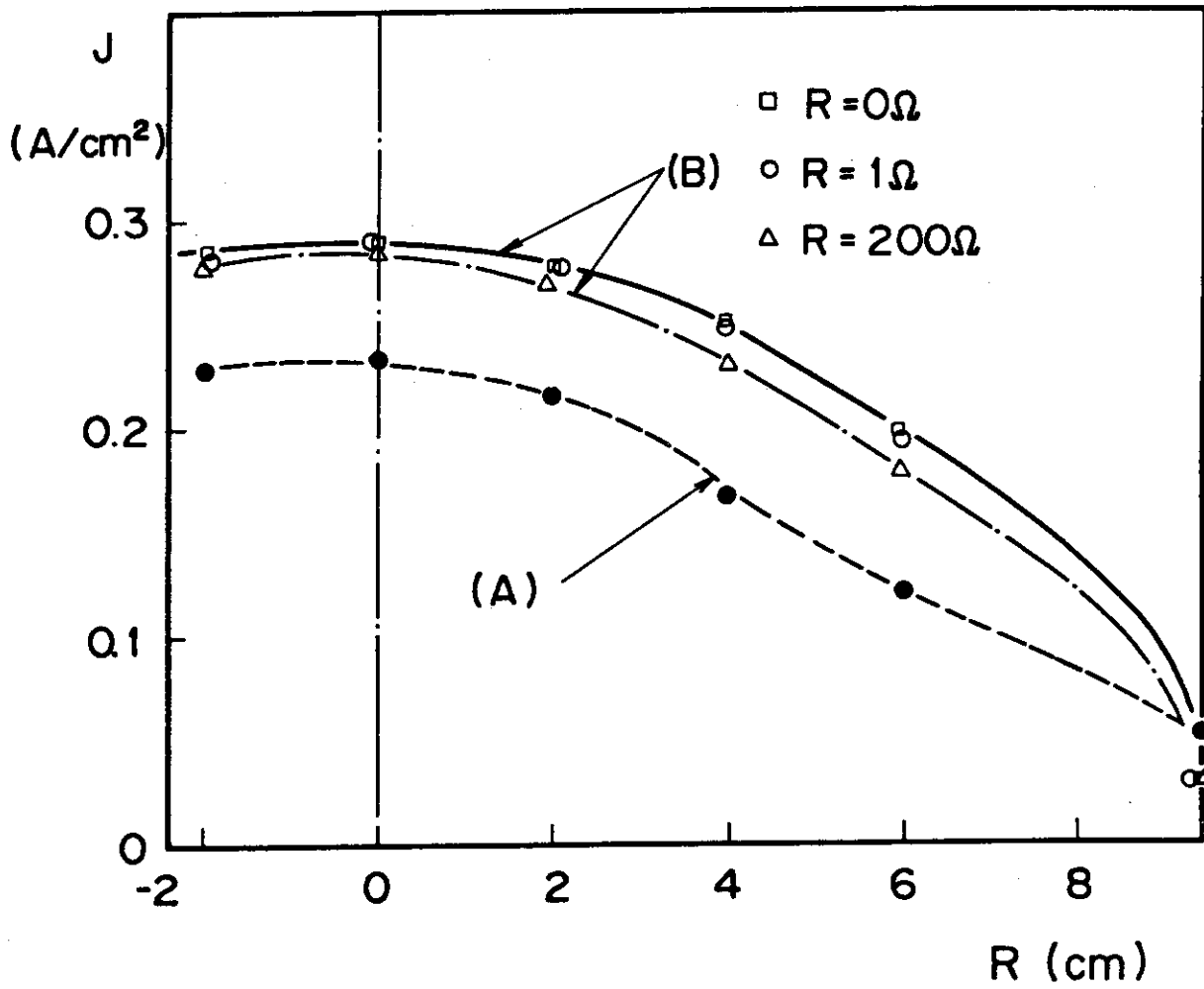
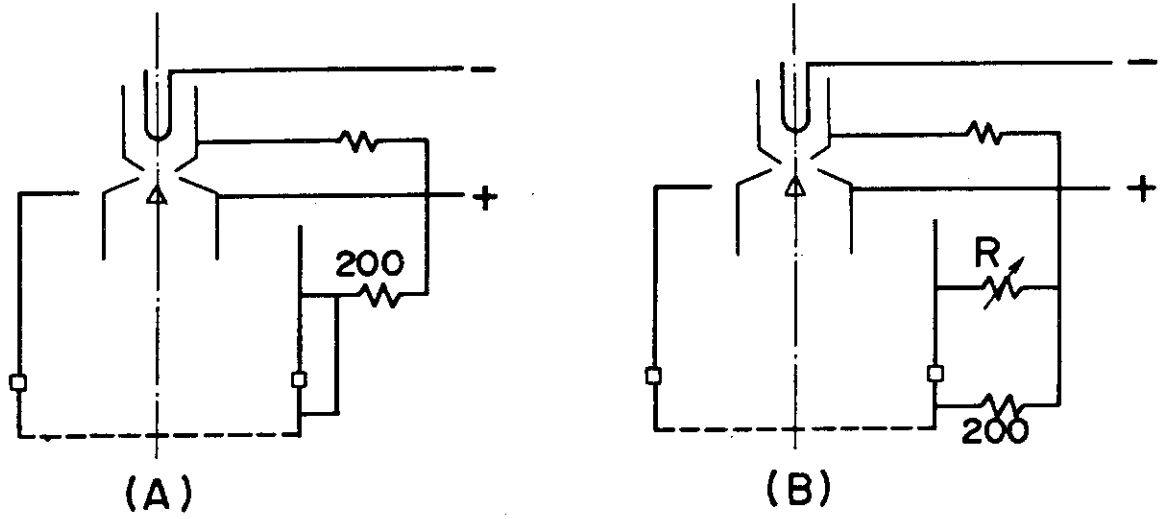


Fig.10 Variations of the density profile with potential of the arc chamber wall.

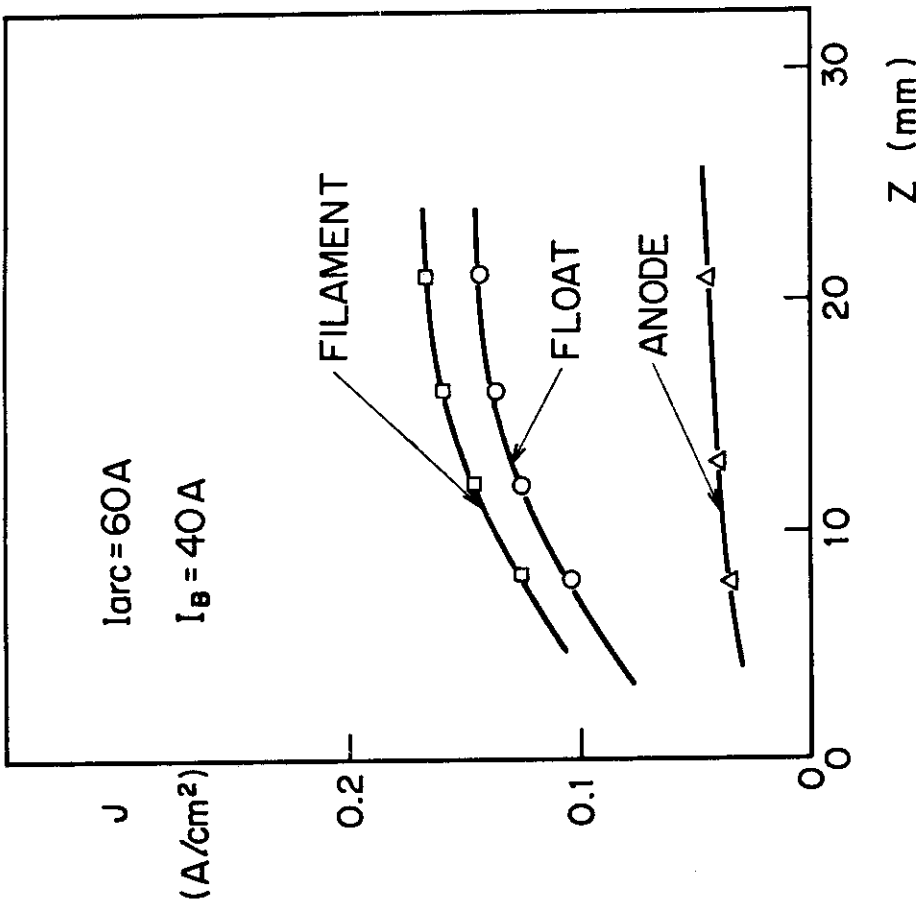


Fig.11 Axial density distributions near the target cathode.

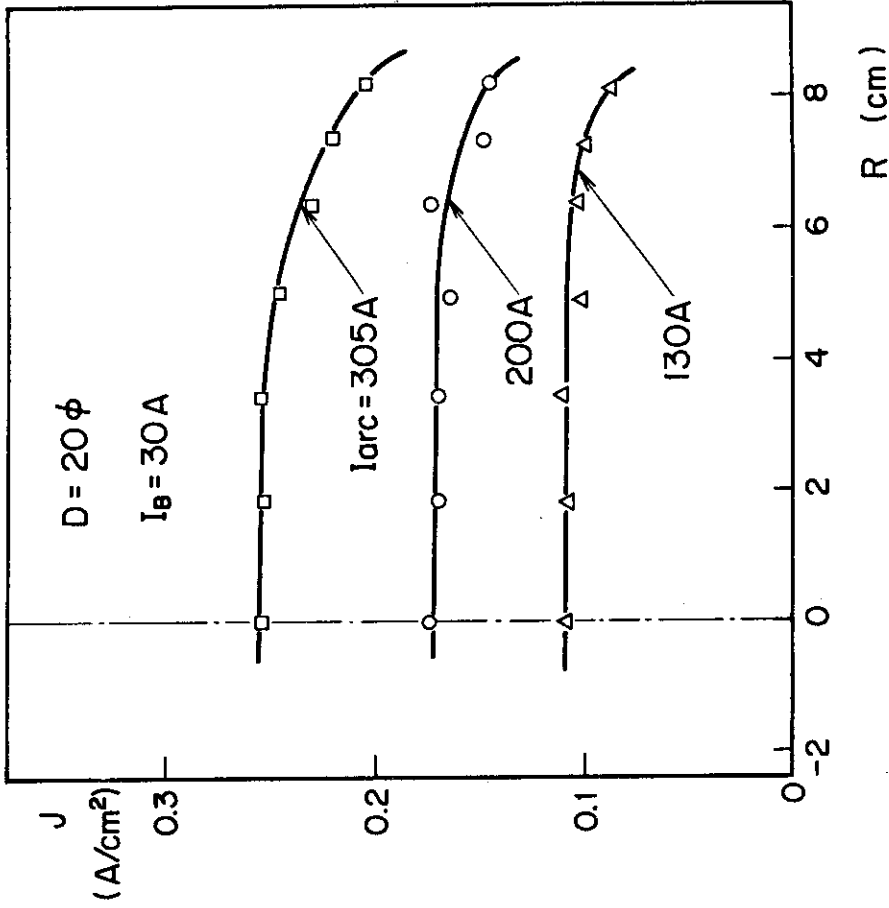


Fig.12 Improved density profiles of the source plasma, where D is the diameter of the intermediate electrode.

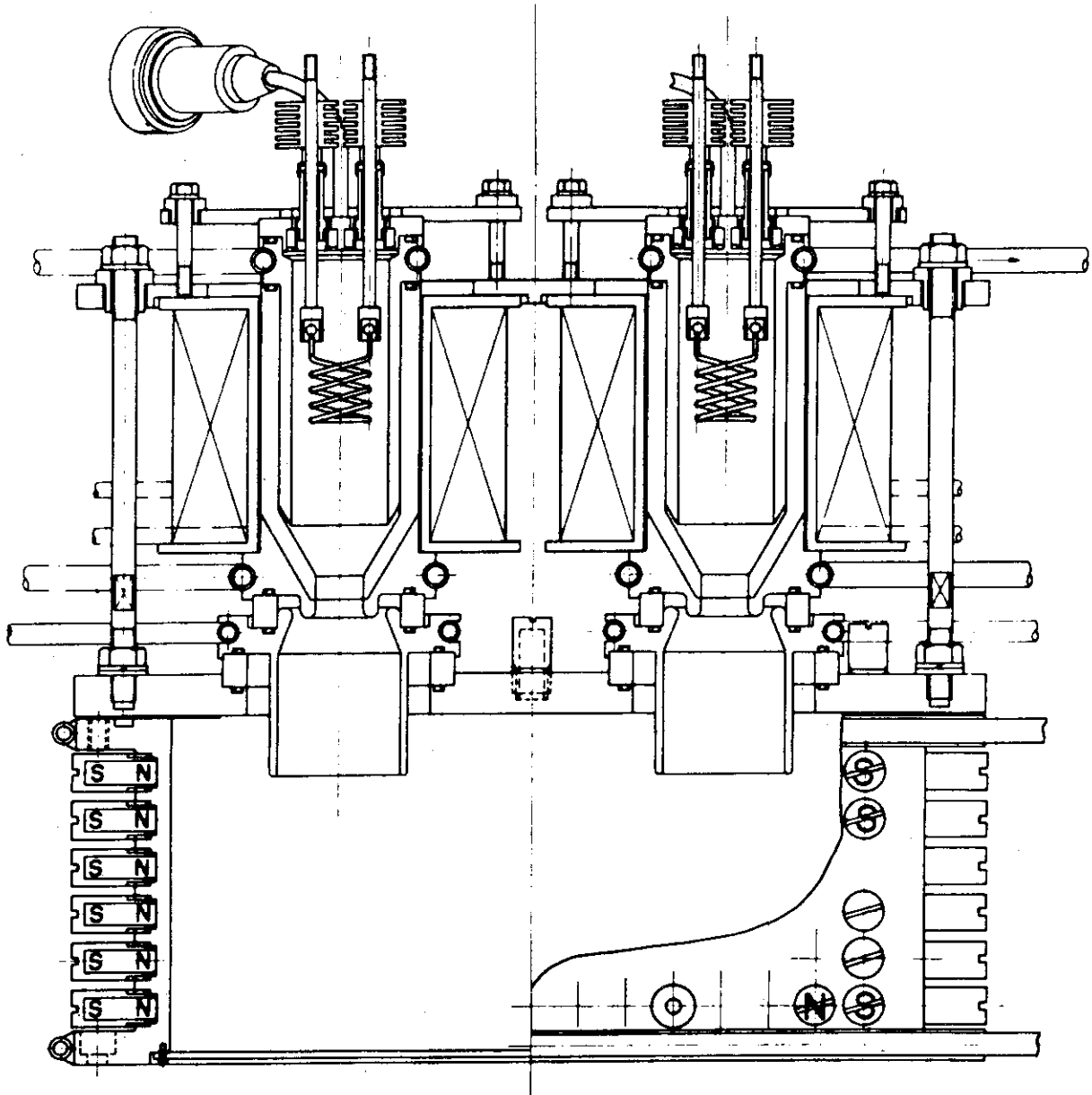


Fig.13 Rectangular plasma source with two duoplasmatrons.

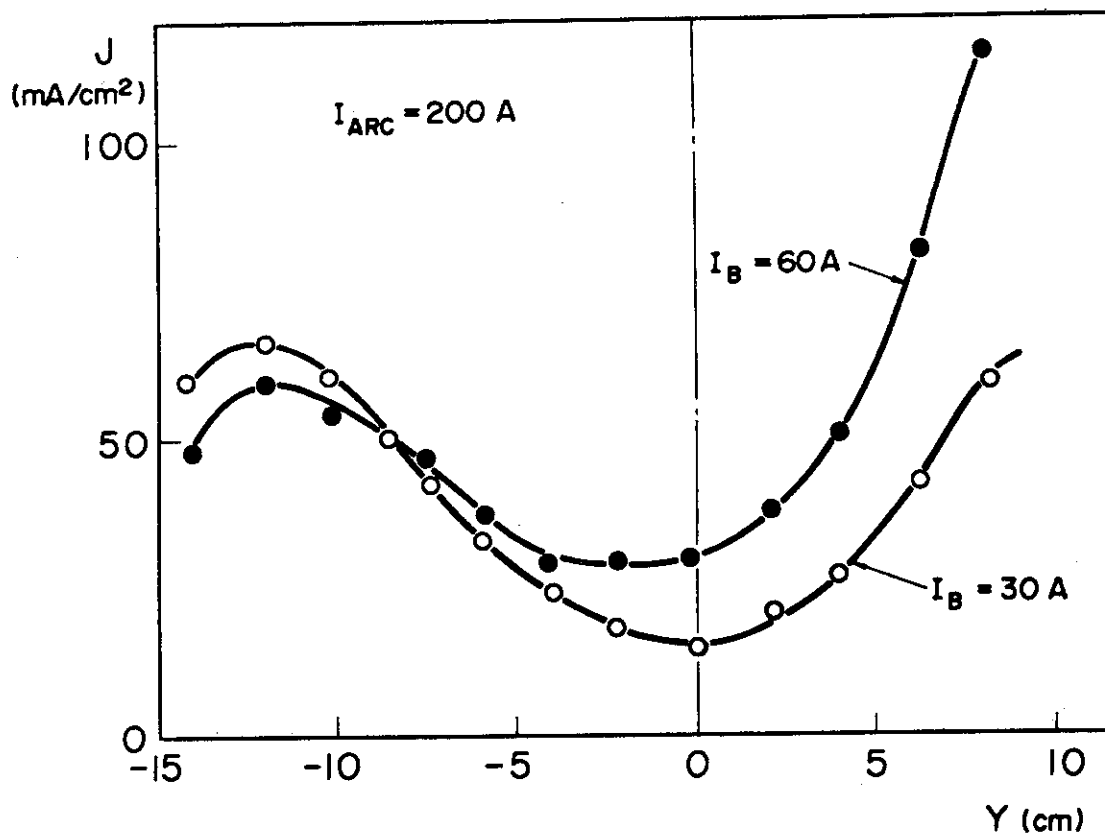


Fig.14 Density profiles of the source with two duoplasmatrons.

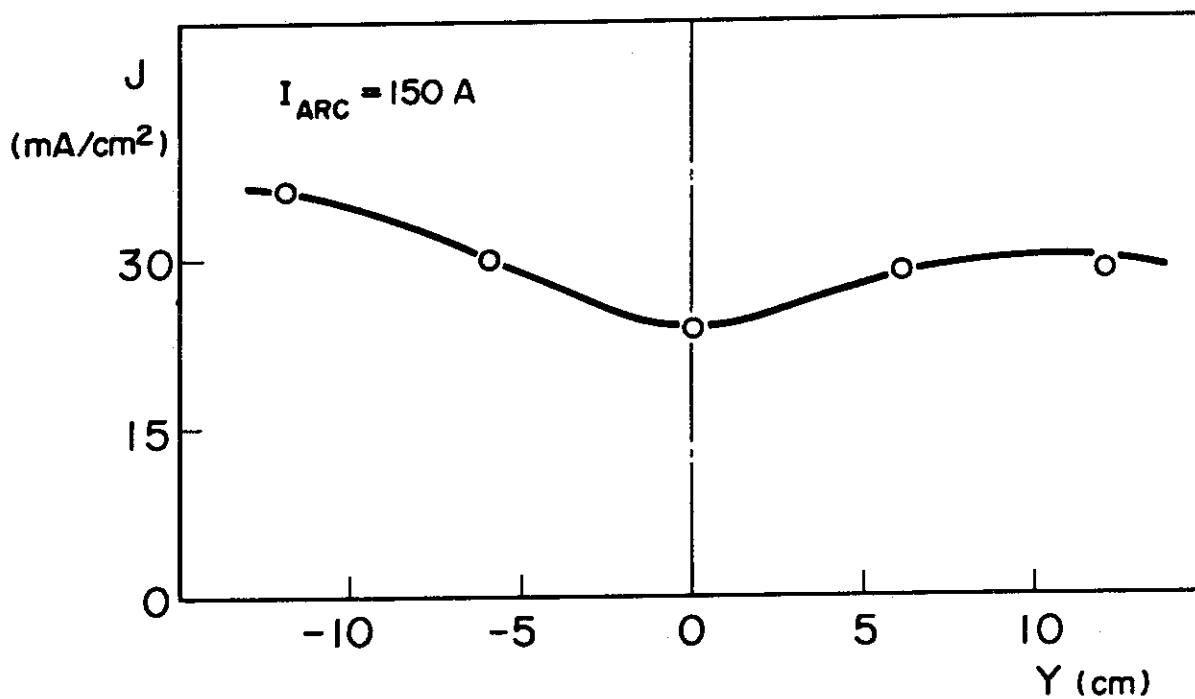


Fig.15 Improved density profile of the source with two duoplasmatrons.

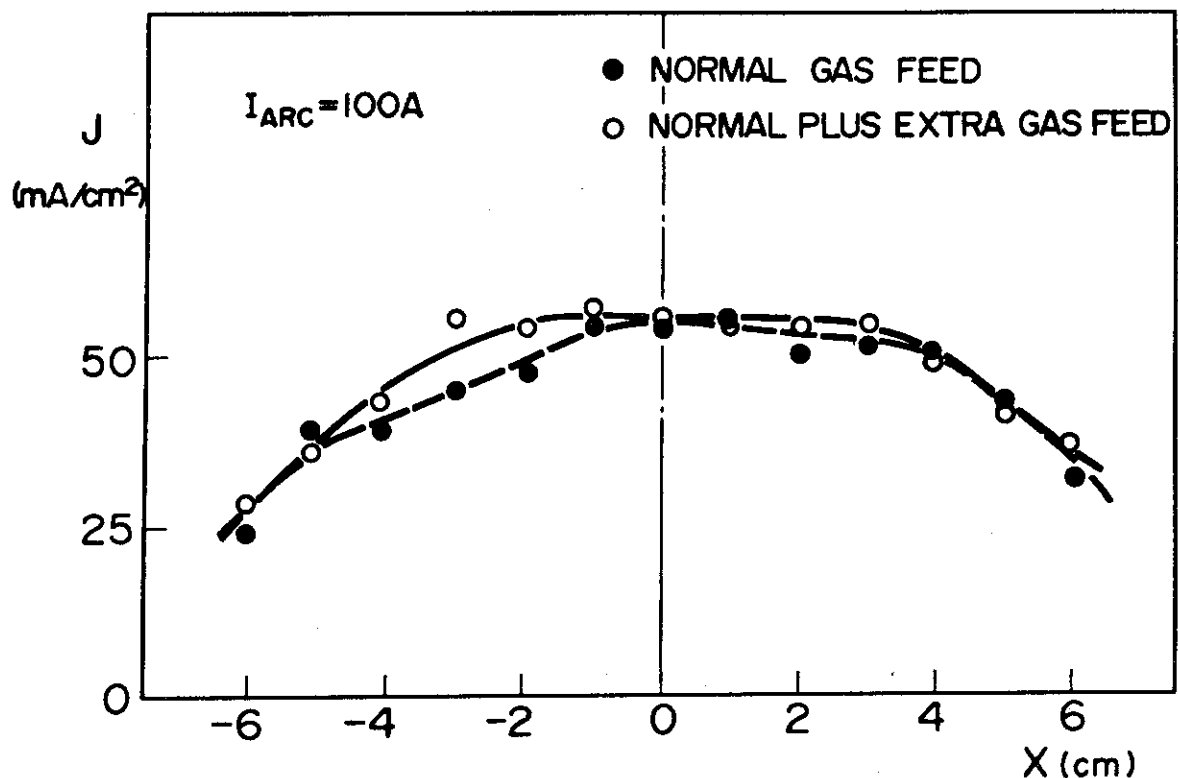


Fig.16 A comparison of the density profiles in the transverse direction with and without extra gas feed.

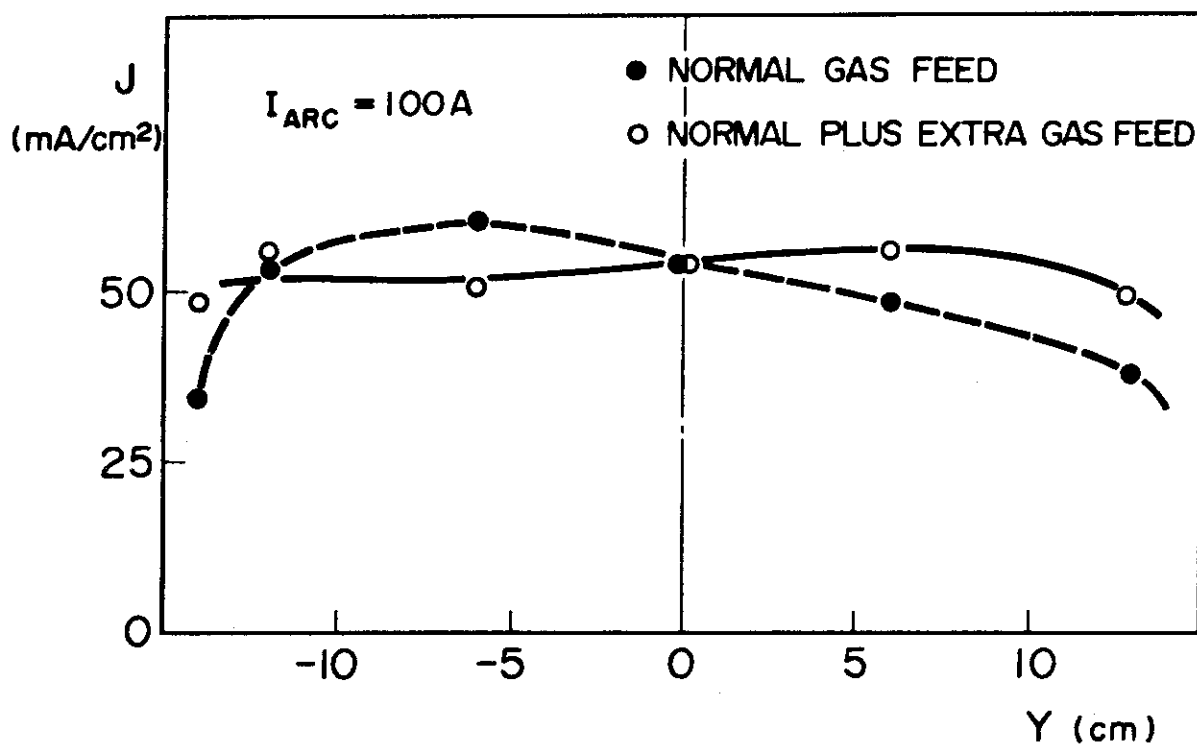


Fig.17 A comparison of the density profiles in the longitudinal direction with and without extra gas feed.

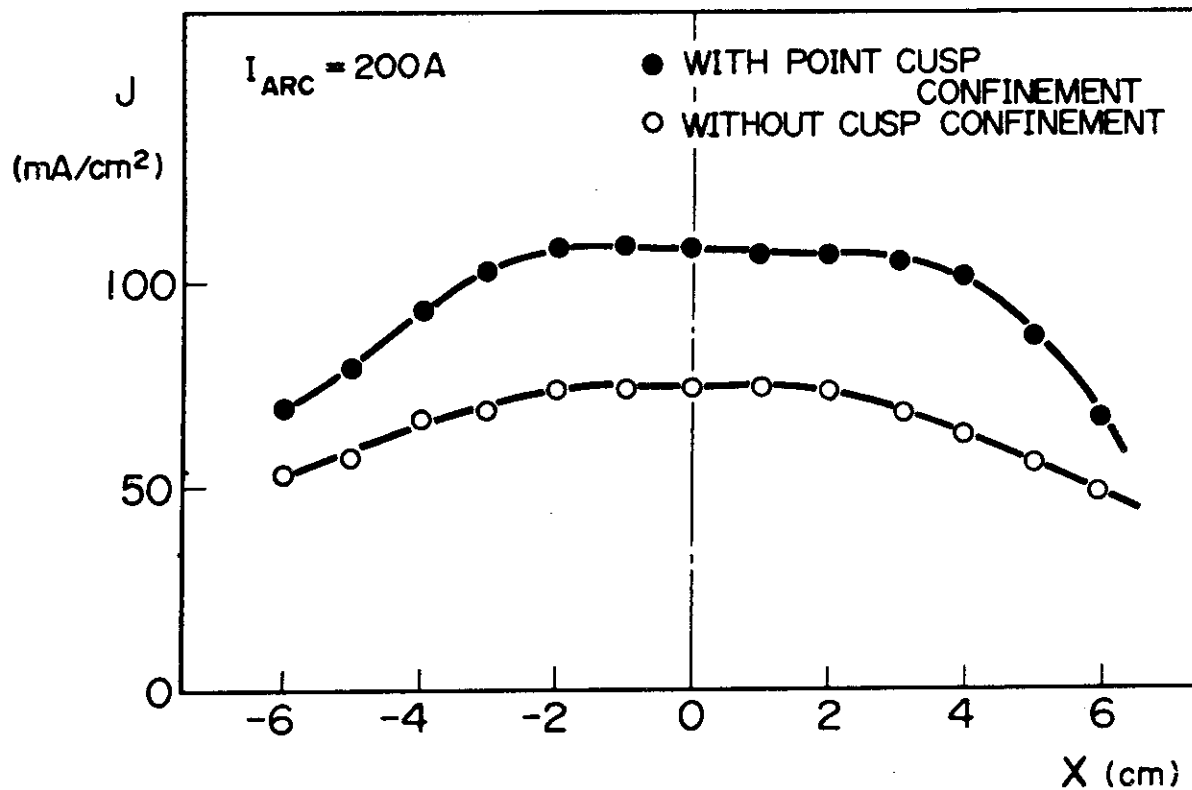


Fig.18 A comparison of the density profiles in the transverse direction with and without point cusp confinement.

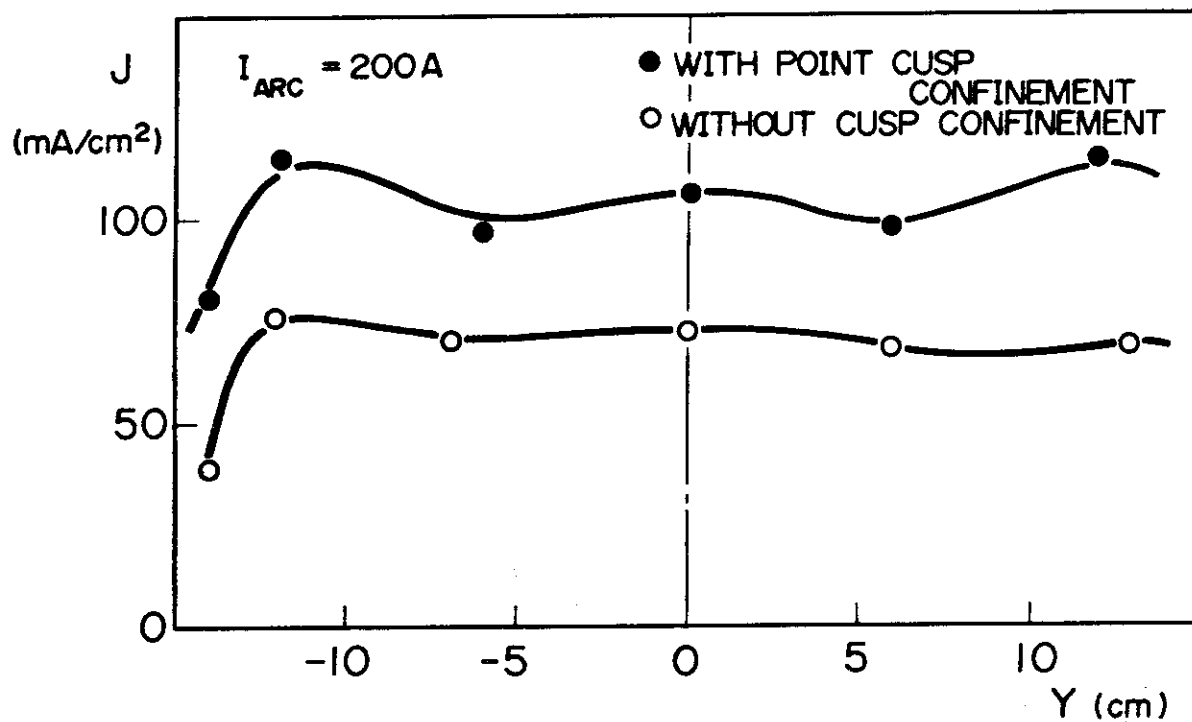


Fig.19 A comparison of the density profiles in the longitudinal direction with and without point cusp confinement.

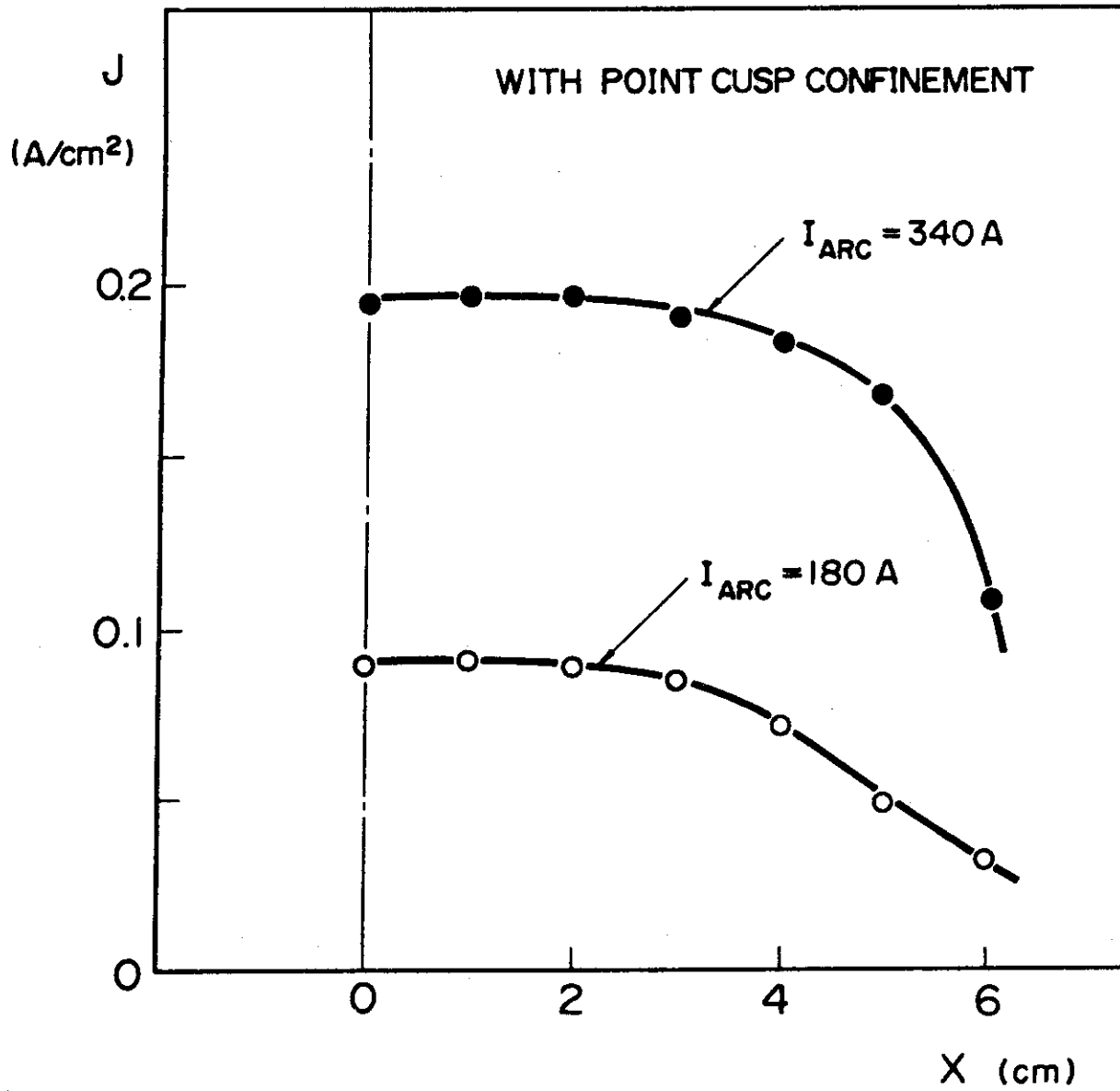


Fig.20 Density profiles of the source by increasing an arc current up to 340 A.